

# Molecular Subtyping Combined with Biological Pathway Analyses to Study Regorafenib Response in Clinically Relevant Mouse Models of Colorectal Cancer



Adam Lafferty<sup>1</sup>, Alice C. O'Farrell<sup>1</sup>, Giorgia Migliardi<sup>2,3</sup>, Niraj Khemka<sup>4,5</sup>, Andreas U. Lindner<sup>4,5</sup>, Francesco Sassi<sup>3</sup>, Eugenia R. Zanella<sup>3</sup>, Manuela Salvucci<sup>4,5</sup>, Evy Vanderheyden<sup>6</sup>, Elodie Modave<sup>6</sup>, Bram Boeckx<sup>6</sup>, Luise Halang<sup>4,5</sup>, Johannes Betge<sup>7,8</sup>, Matthias P.A. Ebert<sup>7</sup>, Patrick Dicker<sup>9</sup>, Guillem Argilés<sup>10</sup>, Josep Taberero<sup>10</sup>, Rodrigo Dienstmann<sup>10</sup>, Enzo Medico<sup>2,3</sup>, Diether Lambrechts<sup>6</sup>, Andrea Bertotti<sup>2,3</sup>, Claudio Isella<sup>2,3</sup>, Livio Trusolino<sup>2,3</sup>, Jochen H.M. Prehn<sup>4,5</sup>, and Annette T. Byrne<sup>1,4,11</sup>

## ABSTRACT

**Purpose:** Regorafenib (REG) is approved for the treatment of metastatic colorectal cancer, but has modest survival benefit and associated toxicities. Robust predictive/early response biomarkers to aid patient stratification are outstanding. We have exploited biological pathway analyses in a patient-derived xenograft (PDX) trial to study REG response mechanisms and elucidate putative biomarkers.

**Experimental Design:** Molecularly subtyped PDXs were annotated for REG response. Subtyping was based on gene expression (CMS, consensus molecular subtype) and copy-number alteration (CNA). Baseline tumor vascularization, apoptosis, and proliferation signatures were studied to identify predictive biomarkers within subtypes. Phospho-proteomic analysis was used to identify novel classifiers. Supervised RNA sequencing analysis was performed on PDXs that progressed, or did not progress, following REG treatment.

**Results:** Improved REG response was observed in CMS4, although intra-subtype response was variable. Tumor vascularity

did not correlate with outcome. In CMS4 tumors, reduced proliferation and higher sensitivity to apoptosis at baseline correlated with response. Reverse phase protein array (RPPA) analysis revealed 4 phospho-proteomic clusters, one of which was enriched with non-progressor models. A classification decision tree trained on RPPA- and CMS-based assignments discriminated non-progressors from progressors with 92% overall accuracy (97% sensitivity, 67% specificity). Supervised RNA sequencing revealed that higher basal *EPHA2* expression is associated with REG resistance.

**Conclusions:** Subtype classification systems represent canonical “*termini a quo*” (starting points) to support REG biomarker identification, and provide a platform to identify resistance mechanisms and novel contexts of vulnerability. Incorporating functional characterization of biological systems may optimize the biomarker identification process for multitargeted kinase inhibitors.

## Introduction

Globally, colorectal cancer is the second most common cancer diagnosis in women and the third most common in men. Twenty-five percent of patients present with metastases at time of diagnosis with a 5-year survival of approximately 10% (1). Mainstay therapy of advanced colorectal cancer involves 5-fluorouracil (5-FU)-based chemotherapy with the addition of targeted agents depending on RAS status (1). Regorafenib (REG) is an orally active multitargeting kinase inhibitor (MKI), which is FDA approved for the treatment of heavily pre-treated chemorefractory patients with metastatic colorectal cancer (mCRC; refs. 2, 3). REG's multipronged mechanism of action includes inhibition of tumor cell proliferation (via MAPK pathway signaling); stimulation of mitochondrial apoptosis through transcriptional activation of PUMA [Bcl-2-binding component 3, isoforms 3/4 (BBC3)]; angiogenesis inhibition through targeting of VEGFR, FGFR, platelet-derived growth factor receptor, and TIE-2 (Angiopoietin-1) receptor; and a reduction in tumor-associated macrophages, an effect possibly mediated through macrophage colony-stimulating factor 1 (CSF1) receptor inhibition (1, 4–8).

In the CORRECT trial REG led to a modest improvement in median overall survival [OS; 6.4 months (REG) vs. 5.0 months (placebo; ref. 2)]. However, a majority of patients experience grade 3–4 adverse events, which frequently prevent treatment continuation (2, 6). Elucidation of predictive/early response biomarkers for better “precision targeting” of REG will likely influence its continued use. Previous attempts to identify such biomarkers have focused on oncogene

<sup>1</sup>Department of Physiology and Medical Physics, Precision Cancer Medicine Group, Royal College of Surgeons in Ireland, Dublin, Ireland. <sup>2</sup>Department of Oncology, University of Torino, Candiolo, Italy. <sup>3</sup>Candiolo Cancer Institute, FPO-IRCCS, Candiolo, Italy. <sup>4</sup>Department of Physiology and Medical Physics, Royal College of Surgeons in Ireland, Dublin, Ireland. <sup>5</sup>Center for Systems Medicine, Royal College of Surgeons in Ireland, Dublin, Ireland. <sup>6</sup>Department of Human Genetics, VIB Center for Cancer Biology, Leuven, Belgium, Laboratory for Translational Genetics, KU Leuven, Leuven, Belgium. <sup>7</sup>Department of Medicine II, Medical Faculty Mannheim, Heidelberg University, Mannheim, Germany. <sup>8</sup>Junior Clinical Cooperation Unit Translational Gastrointestinal Oncology and Preclinical Models, German Cancer Research Center (DKFZ), Heidelberg, Germany. <sup>9</sup>Department of Epidemiology and Public Health Medicine, Royal College of Surgeons in Ireland, Dublin, Ireland. <sup>10</sup>Vall d'Hebron University Hospital and Institute of Oncology (VHIO), Universitat Autònoma de Barcelona, CIBERONC, Barcelona, Spain. <sup>11</sup>UCD School of Biomolecular and Biomedical Science, UCD Conway Institute, University College Dublin, Belfield, Dublin, Ireland.

**Note:** Supplementary data for this article are available at Clinical Cancer Research Online (<http://clincancerres.aacrjournals.org/>).

**Corresponding Author:** Annette T. Byrne, Royal College of Surgeons in Ireland, RCSI Mercer Building, Lower Mercer Street, Dublin 2, Ireland. Phone: 353-1402-8673; Fax: 353-1402-2447; E-mail: [annettebyrne@rcsi.ie](mailto:annettebyrne@rcsi.ie)

Clin Cancer Res 2021;27:5979–92

doi: 10.1158/1078-0432.CCR-21-0818

©2021 American Association for Cancer Research

### Translational Relevance

The effect of regorafenib (REG) treatment on metastatic colorectal cancer patient survival is modest, despite clinical approval. Moreover, treatment is associated with several toxicities, which may diminish quality of life. Elucidation of predictive/early response biomarkers to aid patient stratification will likely influence its use. We have exploited biological pathways studies, using defined molecular subtypes of colorectal cancer as “*termini a quo*” (starting points), to study REG response mechanisms and biomarkers in clinically relevant patient-derived xenograft (PDX) models. We demonstrate the potential for proliferation and apoptosis signatures to predict REG response within consensus molecular subtype (CMS) 4. Application of these signatures is amenable to the molecular pathology setting, and could serve as a stratification tool for REG in the clinic. Protein analysis further revealed cell death-sensitive models that demonstrated improved response to REG treatment. Moreover, we postulate that *EPHA2* expression may be associated with REG resistance treatment irrespective of CMS.

mutations, plasma protein levels, gene expression analysis, circulating tumor DNA, MSI status, and primary tumor location (6, 9–13), but no “single-entity” biomarker has to date been validated for clinical use.

Profiling of complex molecular alterations using unsupervised data-driven approaches has led to new knowledge underpinning colorectal cancer etiology. These data also support the identification of new biomarkers to predict response to targeted therapies (14, 15). For example, we have recently defined a unique mCRC classification system [3 clusters defined by low (cluster 1), intermediate (cluster 2), and high (cluster 3) copy-number burden] based on genome-wide distribution of copy-number alterations (CNA) in colorectal cancer tumors, and have identified copy-number load as a novel predictive biomarker of bevacizumab combination therapy (14). A major effort has also focused on reclassifying colorectal cancer based on tumor expression data, resulting in a new colorectal cancer consensus molecular subtype (CMS) classification system, which defines a “consensus” for transcriptomic subtyping of colorectal cancer (16). The marked interconnectivity between independent gene expression classifiers obtained by unsupervised clustering approaches gave rise to the four CMS groups, which as we have recently discussed, not only reflect cancer cell phenotypes but also microenvironment features present in bulk tumor samples (17, 18). For example, CMS4 tumors have significant enrichments for VEGF signaling, which is a target of approved therapies in the metastatic setting, including bevacizumab and REG. In this context, the biological hypothesis is that patients with mesenchymal–stromal CMS4 tumors are particularly sensitive to anti-angiogenic agents. The prognostic value of CMS subtypes has also recently been confirmed in the metastatic setting (18).

Interestingly, retrospective exploratory analysis of the CORRECT trial to evaluate the clinical benefit in colorectal cancer subgroups suggests a differential response to REG across CMS subtypes (data presented in Poster #3558, ASCO 2015; ref. 19). These hypothesis-generating data suggested that CMS2 and CMS4 subtyped patients received the greatest OS benefit from REG [Hazard ratios (HR) 0.779 and 0.672, respectively], compared with CMS3 and CMS1 patients (HRs, 1.047 and 1.116, respectively). However, even in the confined setting of CMS2 or CMS4, REG response is variable, and not all patients of a given subtype respond to treatment (19, 20). Indeed in general, the CMS classification does not currently provide a rationale

for therapy selection in mCRC (21). Moreover, technical issues that lead to misclassification of colorectal cancer samples, as well as biological factors related to spatial and temporal intratumor heterogeneity are likely to have an impact on the results of studies assessing interactions between CMS groups and treatment effects (21).

We hypothesized that analysis of signaling pathways within subtypes may provide novel insights into REG responses and may explain response heterogeneity. To achieve these objectives, we used a faithful preclinical patient-derived xenograft (PDX) platform of rationally selected subtyped tumors, which accurately recapitulate the observed (modest) clinical treatment response. Within these models, CMS and CNA classifiers were used as a starting point to (i) determine whether known REG-targeted cancer hallmarks (angiogenesis, proliferation, and apoptosis) had potential biomarker utility to support better precision targeting of REG within subtypes and (ii) to provide hints toward novel contexts of vulnerability and future REG combination approaches. Finally, to identify putative resistance mechanisms, we studied differential gene expression signatures in PDX models that progressed following REG treatment versus non-progressors.

## Materials and Methods

### Compliance with ethical standards and REG treatment

*In vivo* studies performed at University College Dublin were approved by UCD Animal Research Ethics Committee and work performed under Health Products Regulatory Authority license number AE18982/P076. *In vivo* studies performed at the Candiolo Cancer Institute were approved by the Internal Ethical Committee and the Italian Ministry of Health. Female NOD/SCID mice were purchased from an approved supplier (Charles River laboratories) and were ages between 4 and 6 weeks. In both institutes, animals were housed in individually ventilated cages in a 12-hour light/dark cycle at 22°C. Animals were provided with *ad libitum* access to food and water and suitable environmental enrichment. Mice were anesthetized using 1%–2.5% isoflurane/1L/min O<sub>2</sub> for the duration of all described procedures. In all experiments, mice received 10 mg/kg of REG [reconstituted in propylene glycol/PEG400/Kolliphor P188 (Sigma), 42.5/42.5/15 + 20% H<sub>2</sub>O], orally, daily. Treatment was for 28 days unless otherwise described, or until humane endpoint based on tumor size, defined in the ethical approval. Tumor growth was evaluated up to three times weekly, using caliper measurements.

### mCRC PDX population trial

PDXs derived from liver metastases of 43 treatment-naïve or chemorefractory patients with mCRC that represented the global molecular and genetic landscape of the human disease population were selected from the PDX biobank at the Candiolo Cancer Institute. The distribution of somatic mutations in the cohort was: wild-type,  $n = 16$  (37.2%); *KRAS*mut,  $n = 18$  (41.8%); *BRAF*mut,  $n = 5$  (11.62%); *NRAS*mut,  $n = 3$  (6.9%). PDXs had previously been categorized into CMS subtypes using gene expression data from the patient tumors from which they were derived [available from the GEO database (NCBI) with accession number GSE73255; refs. 22, 23] and following methods outlined for the CMScaller package (24). Propagation, implantation, and passaging (to a maximum of 10 passages) of tumor material was performed also as previously described (25). A “one animal per treatment” ( $1 \times 1 \times 1$ ) experimental design was adopted (i.e.,  $n = 3$  mice per PDX model). When PDX tumor volumes reached approximately 400 mm<sup>3</sup> [calculated using the formula  $4/3\pi \cdot (d/2)^2 \cdot D/2$ , where  $d$  is the minor tumor axis and  $D$  is the major tumor axis] mice were randomly assigned to respective groups (pre-treatment, vehicle,

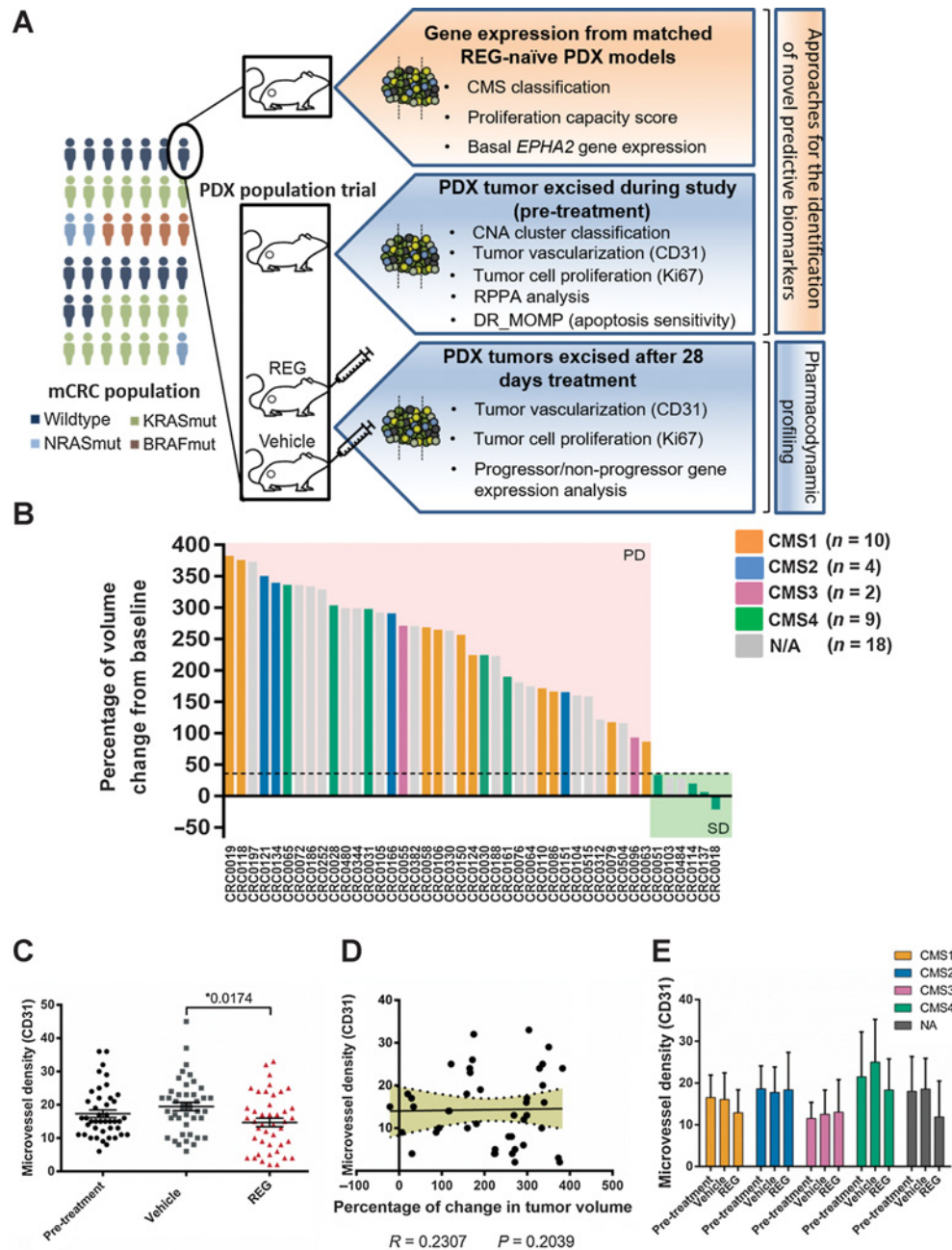


**Figure 1.**

REG exerts a heterogeneous antitumor effect in PDX models and leads to a CMS independent decrease in CD31 staining. **A**, Overview of the PDX population trial experimental workflow and downstream analyses. The PDX tumor cohort represents the global mutational incidence and CMS subtypes 1–4. The percentage of PDX mutation status are as follows: wild-type (37%), *KRAS*mut (41%), *NRAS*mut (6.9%), *BRAF*mut (11%). Historic gene expression data (generated from the same PDX models, available at GSE76402) has been used to classify the PDX models into CMS subtype. For the PDX population trial, a “one animal per treatment” ( $1 \times 1 \times 1$ ) experimental design was undertaken (i.e.,  $n = 43$  PDX models,  $n = 3$  mice per PDX model). Following implantation tumors were allowed to grow until they reached 400 mm<sup>3</sup>. One REG-naïve tumor was then harvested for pre-treatment analysis, whereas the 2 remaining tumor-bearing mice were treated with either REG or vehicle for 28 days. **B**, Waterfall plot of REG response (in  $n = 43$  PDX-bearing mice treated with REG; 10/mg/kg/d) after 4 weeks of treatment. Tumor volume at 28 days was normalized to baseline (i.e., tumor volume on the day that treatment commenced). Dotted line indicates the cutoff value for defined categories of therapy response using mRECIST criteria: cases displaying disease progression (“PD” >35% increase in tumor volume) or stabilization (“SD” <35% increase in tumor volume). **C**, CD31 staining of pre- and post-treatment tumor material reveals that after 4 weeks, REG-treated tumors have a lower MVD (percentage of CD31 positivity of the total area) compared with vehicle-treated tumors ( $n = 43$  vehicle,  $n = 43$  REG,  $P = 0.0174$ ) in MVD density. **D**, Post-treatment CD31 expression does not correlate with changes in PDX tumor volume. **E**, REG effects on mean MVD density are not specific to CMS subtypes. Mean is presented for each subtype (CMS1  $n = 10$ , CMS2  $n = 4$ , CMS3  $n = 2$ , CMS4  $n = 9$ , N/A  $n = 18$ ). Error bars indicate SEM.

Downloaded from <http://aacrjournals.org/clinccancerres/article-pdf/27/21/5979/2989559/5979.pdf> by guest on 09 March 2022

REG). The REG-naïve tumor was immediately harvested for pre-treatment analysis, whereas the 2 remaining tumor-bearing mice were treated with either REG or vehicle. Following excision of tumors (pre- and post-treatment), half was formalin fixed for IHC analyses, one quarter of the tumor was flash-frozen [FF (for protein and low coverage whole-genome sequencing (LC-WGS)], and the remaining tissue preserved in RNAlater for transcriptomic profiling. Gene expression data from REG-naïve PDX tumors (matching those used in the population trial) were also available for basal gene expression analyses [data were retrieved from the GEO database (NCBI) with accession number GSE76402 (refs. 22, 23)]. Please refer to Fig. 1A for details on experimental design.

#### Assignment of mCRC PDX models to CNA subtypes

Assignment of the PDX models to CNA subtype (using the harvested REG-naïve pre-treatment mCRC PDX tumors), including the preparation of shotgun whole-genome libraries and LC-WGS, was performed as previously described (14). GISTIC (26) v2.027 (RRID:SCR\_000151) was used to identify the most frequent and overrepresented chromosomal aberrations in tumors according to previously defined parameters. Significantly amplified or deleted regions were assigned as homozygous deletion, loss, diploid, gain, or amplification for each sample based on LogR signal and GISTIC output threshold values ( $t < -1.3$ ;  $-1.3 \leq t < -0.1$ ;  $-0.1 \leq t \leq 0.1$ ;  $0.1 < t \leq 0.9$ ;  $t > 0.9$ , respectively).

#### IHC

Pre-treatment tumor and tumors excised following 28 days of treatment with REG or vehicle in the PDX population trial were studied. Half of the material from each tumor was formalin fixed and processed for IHC analysis. IHC was performed using DAB probes for Proliferation marker protein Ki-67 (1:100; Cell Signaling Technology, Cat# 9449S, RRID:AB\_2715512) and CD31 [Platelet endothelial cell adhesion molecule (PECAM-1; 1:100, Cell Signaling Technology, Cat#3528, RRID:AB\_2160882)]. Sections were deparaffinized and endogenous peroxidase activity was blocked using 3% H<sub>2</sub>O<sub>2</sub>. Slides were blocked for 10 minutes in an UltraVision blocking agent. Primary antibody was applied and incubated at room temperature for 1 hour. Slides were subsequently incubated for 20 minutes in primary antibody enhancer. Sections were then incubated in horseradish peroxidase (HRP) for 15 minutes and DAB for 10 minutes and counterstained in hematoxylin before dehydration in ascending gradient alcohols and xylene before mounting. Slides were imaged using a light microscope and images taken at  $\times 40$ . Tumor tissue sections (center areas of each section) were analyzed using ImageJ (National Institutes of Health, RRID:SCR\_003070; ref. 27), which segmented cells with positive and negative staining. The percentage of the area containing positive cells was calculated as the brown area (positively stained cells) divided by the sum of brown and blue areas (negatively stained cells)\*100. The software interpretation was manually verified by visual inspection of the digital images to ensure accuracy.

#### Proliferation capacity

Historical REG-naïve PDX gene expression data (i.e., previously collated data from the same PDX models as used in the current study, available at GSE76402) were used to calculate the proliferation capacity of each model. Analysis was as previously described (Supplementary Methods in Nielsen and colleagues; ref. 28), done by averaging the normalized gene expression values of an 11-gene signature [BIRC5, CCNB1, CDC20, CDCA1 (NUF2), CEP55, NDC80, MKI67, PTTG1, RRM2, TYMS, and UBE2C].

#### Western blotting

FF PDX tumor specimen pellets collected in the PDX population trial were directly homogenized and mixed with lysis buffer containing 0.5 mmol/L Tris-HCl (pH 6.8), 10% glycerin (w/v), 2% SDS (w/v), and protease and phosphatase inhibitor cocktails (Roche). Protein concentration was determined with the Pierce 660 nm reagent assay (Pierce) and a total of 30  $\mu$ g of protein loaded into an SDS gel after complete denaturation at 90°C for 10 minutes in Laemmli buffer. The samples were then transferred to nitrocellulose membrane and blocked in 5% milk in TBST for 1 hour. Primary antibodies to MCL-1 (1:1,000; BD Biosciences Cat# 559027, RRID:AB\_397176), BCL-2 (1:100; Santa Cruz Biotechnology, Cat# sc-509, RRID:AB\_626733), BCL-xL (1:1,000; Cell Signaling Technology, Cat# 2762, RRID:AB\_10694844), EPHA2 (1:1,000; Invitrogen Cat# 37-440, RRID:AB\_2533318), and actin (1:5,000; Sigma-Aldrich, Cat# A3853, RRID:AB\_262137) were mouse monoclonal. Antibodies to BAK (1:250; Santa Cruz Biotechnology, Cat# sc-517390) and BAX (1:1,000; Cell Signaling, Cat# 2772, RRID:AB\_10695870) were rabbit polyclonal. The HRP-conjugated secondary antibodies were from Jackson ImmunoResearch (1:5,000). Detection of protein bands was carried out using chemiluminescence (EMD Millipore) on a LAS3000 Imager (FUJIFILM UK Ltd. System). For quantitative analysis (input to DR\_MOMP) BCL-2 profiling and absolute protein concentration was performed as previously described through quantitative Western blotting (29).

#### Calculation of the sensitivity of tumor cells to undergo apoptosis using the DR\_MOMP computational tool

The tumor cells' sensitivity to undergo apoptosis was calculated using the ordinary differential equation (ODE)-based systems model DR\_MOMP (29). This extensively validated computational tool is comprised of 126 reactions and 71 protein species that delivers a numeric score indicative of the sensitivity of cancer cells to undergoing mitochondrial apoptosis (via membrane outer mitochondrial permeability, MOMP). A full description of DR\_MOMP and relevant methodology has been previously been described (Lindner and colleagues; ref. 29). Absolute protein levels of BAK, BAX, BCL-2, BCL-xL, and MCL-1, measured in the harvested FF REG-naïve tumor material using Western blot analysis, were used to calculate the genotoxic stress dose that induces MOMP ("stress-dose"). Protein production, degradation, and BCL2 interactions were modeled by a pseudo-reaction network using mass action kinetics, translated into a set of ODEs and solved using the MATLAB 7.3 (The MathWorks, R2007b, 7.5.0.342, RRID:SCR\_001622) function ode15s.

#### Reverse phase protein array analysis

Protein was extracted from the harvested FF REG-naïve pretreatment PDX tumor tissue and from HeLa cell line standards. Reverse phase protein array (RPPA) was performed as previously described (20). Protein lysates were normalized to 1  $\mu$ g/ $\mu$ L as assessed by bicinchoninic acid assay (BCA, Bio-Rad). A panel of 72 antibodies targeting various key cancer-related proteins was used for measuring protein levels (see Supplementary Table S1 for a full list of antibody information). The DAKO (Carpinteria) catalyzed signal amplification system was used for antibody blotting. Each slide was incubated with a primary antibody. RPPA data were scaled across the samples for data analysis. Only RPPA data with a coefficient of variation (CV) in the range 0.25–2.5 were considered for analysis. Unsupervised clustering was performed using the consensus clustering algorithm from Cancer-Subtypes (v1.12.1) R package using parameters (clusterAlg = "hc," distance = "spearman"; ref. 30). RPPA clusters were annotated with

treatment response and assignments to CMS subtype and copy-number cluster. PAMR (v1.56.1; ref. 31) and SAMR (v3.0; ref. 32) R package were used to identify protein predicting response to treatment. A classification decision tree was fitted using as input the assignments for CMS subtype and RPPA cluster to predict response to REG treatment [stabilization (non-progressor) vs. progression]. Model development and visualization was performed with the rpart (version 4.1–15) and rpart.plot (version 3.0.9) R packages.

### Transcriptomic analysis of non-progressors and progressors following REG treatment

#### Transcriptomic analysis of post-treatment PDX models

Tumor material, preserved in RNAlater, excised after 28 days of treatment, from the 6 mice that responded best to REG treatment (“non-progressors,” i.e., models exhibited growth stabilization upon REG treatment) and 3 mice that responded the least (“progressors”) in the PDX efficacy study were selected for transcriptomic analysis. RNA was extracted from the PDX material using TRIzol/chloroform and the RNeasy Mini Kit (Qiagen). Quantity and quality of RNA were assessed by Nanodrop and Experion (Bio-Rad). mRNA enrichment and library preparation were performed using the TruSeq mRNA sample preparation kit v2 (Illumina), as per the manufacturer’s instructions. RNA sequencing was performed using Illumina HiSeq2000 as previously described (33). One non-progressor PDX model was excluded due to low raw read counts. Therefore, 5 non-progressors ( $n = 3$  CMS4,  $n = 2$  unclassified) and 3 progressors (all CMS1) were analyzed for differential gene expression.

Differential expression analysis was performed using the DESeq2 package [(RRID:SCR\_015687; ref. 34) in the R statistical environment (ref. 35) R Development Core Team, RRID:SCR\_001905]. A “conditions” data frame was created on the basis of the sample names, their group, and their sensitivity to therapy. Counts and condition data frames were loaded into a DESeq2DataSet class object using the *DESeqDataSetFromMatrix()* call, with the design variable set as “approximately group.” Volcano plots and heatmaps were generated using EnhancedVolcano and Heatmap2 packages in R.

#### Data mining of historical treatment-naïve tumor gene expression data

To determine whether targets that were differentially expressed at treatment end point were also differentially expressed at basal (i.e., untreated) level, the previously described publicly available expression dataset (GSE76402) was mined using a supervised approach.

#### Statistical analysis

Treatment response in PDXs was assessed by calculating the percentage of increase in tumor volume for each model and characterizing the change in volume according to mRECIST criteria (36). One-way ANOVAs with Tukey’s *post hoc* multiple comparisons were used to determine significance in IHC. For RPPA analysis, differences in protein levels between clusters were identified by one-way ANOVA with subsequent Tukey’s *post hoc* tests. Correlations were assessed by fitting a linear regression to the data. Correlations and 95% confidence intervals were calculated using Pearson’s correlation analysis in GraphPad Prism 7 (La Jolla, RRID:SCR\_002798; ref. 37). Other statistical analyses were also performed using GraphPad Prism 7. Unless otherwise stated,  $P$  values  $\leq 0.05$  were considered statistically significant.

## Results

### Analysis of REG response in subtyped PDX models reveals CMS4 sensitivity

As described, PDX models were chosen to represent the global molecular and genetic landscape of the human disease population (Fig. 1A). Treatment response to REG in a clinically relevant panel of  $n = 43$  molecularly characterized PDX tumors was evaluated (Fig. 1B). Treatment response was characterized according to mRECIST criteria (36). Six PDX models displayed tumor growth stabilization (defined as “non-progressors”  $<35\%$  increase in tumor volume) whereas 37 displayed progressive disease (defined as “progressors,”  $>35\%$  increase in tumor volume). No PDX models displayed either a complete ( $< -95\%$  decrease in tumor volume) or partial ( $< -50\%$  decrease in tumor volume) response.

When analyzed in the context of CMS subtype, of the 37 models that progressed under treatment, 10 were CMS1, 4 CMS2, 2 CMS3, 5 CMS4 and 16 were unclassified [assignment of samples into CMS subtypes failed; as described by Guinney and colleagues (ref. 16) non-consensus samples are likely mixtures of one or more subtype or of indeterminate subtype]. Of the 6 non-progressor models (i.e., disease stabilization was apparent), 4 were CMS4 whereas 2 were CMS-unclassified (Fig. 1B). Thus in PDXs, as in patients, response to REG treatment is heterogeneous, even within the CMS4 subtype.

We applied our previously described CNA classifier (12) to the PDX cohort. Data revealed that CNA high cluster 3 was highly represented (22 models). Fourteen models were CNA intermediate cluster 2 and 4 were CNA low cluster 1. Four PDX models were not available for copy-number analysis due to failed quality metrics. When analyzed in the context of response to REG treatment, of the 33 CNA-classified models that progressed, 3 were CNA low cluster 1, 13 were CNA intermediate cluster 2, and 17 were CNA high cluster 3. Of the 6 non-progressor models (i.e., evident disease stabilization), 5 were CNA high cluster 3 and 1 was CNA intermediate cluster 2 (Supplementary Fig. S1). Again, intra-subtype heterogeneity in response was evident. Consequently, more detailed pathway studies were undertaken, using the clinically relevant PDX model platform to interrogate observed subtype-specific effects using functional and systems-based analyses.

### Analysis of the subtype-specific treatment effects on tumor vasculature in PDX models

Angiogenesis is an established REG target. To explore the anti-angiogenic effects of REG in selected PDX models, we investigated tumor microvessel density (MVD) using mouse-specific CD31. We further examined the relationship between pre-treatment tumor vasculature and treatment outcome. IHC was performed on half of each tumor taken at pre-treatment and at the end-point of the PDX population trial. After 28 days, REG-treated tumors had significantly reduced endothelial expression of CD31 across all PDX tumors, compared with vehicle-treated tumors [Fig. 1C; mean MVD  $18.74 \pm 1.17$  SEM (vehicle),  $14.62 \pm 1.06$  SEM (REG),  $P = 0.0174$ ]. No change compared with pre-treatment tumors was observed. There was no significant correlation between post-treatment MVD (Fig. 1D) or pre-treatment MVD (data not shown) and change in tumor volume, following REG treatment. When analyzed by CMS subtype, no significant effects on MVD were apparent (Fig. 1E). A non-significant trend toward decreased MVD following REG treatment in CMS4 subtyped and unclassified PDXs was observed. When analyzed in the context of CNA clusters, REG significantly attenuated MVD in CNA low cluster 1 ( $P = 0.0286$ ), although the authors note the low sample size in this group, limiting

conclusions. MVD had no significant effect on CD31 expression in CNA intermediate cluster 2 or CNA high cluster 3 (Supplementary Fig. S2A).

### Gene-based proliferation signature predicts favorable REG response in CMS4 models

REG prevents the phosphorylation of intracellular moieties that are often involved in the processes of cell proliferation via targeting of multiple active kinome sites. Thus, we next sought to interrogate the antiproliferative effect of REG in the context of CMS and CNA subtypes. We also examined whether pre-treatment proliferation was correlated with treatment outcome. Available pre- and post-treatment REG ( $n = 38$ ) and vehicle ( $n = 38$ ) FFPE PDX material was stained for human-specific Ki-67 to determine proliferation indices. Following 28 days of treatment, Ki-67 was significantly decreased in REG compared with vehicle-treated tumors when the entire PDX cohort was evaluated [mean proliferation index  $47.391 \pm 1.875$  SEM (vehicle),  $40.979 \pm 2.046$  SEM (REG)  $P = 0.0386$ ; Fig. 2A]. Analysis of post-treatment Ki-67 expression revealed no significant correlation with changes in tumor volume following REG treatment [ $R = 0.1351$ ,  $P = 0.4186$ ; Fig. 2B (post-treatment); pre-treatment data not shown]. When analyzed in the context of CMS, REG significantly reduced

proliferation in CMS1 tumors ( $P = 0.0108$ ; Fig. 2C). We observed a non-significant trend toward decreased proliferation in CMS2, 3, and 4 tumors ( $P = 0.2624$ ,  $P = 0.0502$ , and  $P = 0.0931$ , respectively; Fig. 2C). REG did not differentially affect proliferation in tumors when analyzed in the context of CNA clusters (Supplementary Fig. S2B).

Next, using the publicly available transcriptomics data from the same PDX models (i.e., REG-naïve cohort, transcriptomics data available at GSE76402), we investigated whether a proliferation capacity score, determined by the application of an established 11-gene “proliferation signature” (28) to each PDX model, could predict REG treatment outcome. The proliferation capacity score was determined by averaging the normalized gene expression values measured in each pre-treatment tumor. Across the entire PDX cohort, no relationship between proliferation capacity score and tumor response to REG was evident (data not shown). When analyzed in the context of CMS subtype, no significant correlation was observed between proliferation capacity score and response to REG in CMS1 or CMS2 (Pearson; CMS1;  $R = -0.5335$ ,  $P = 0.1390$ ; CMS2;  $R = -0.7527$ ,  $P = 0.2473$ ; Fig. 2C). The ability of proliferative capacity score to predict REG response could not be analyzed in the CMS3 subtype due to a low number of CMS3 PDX tumors. However, a significant linear correlation was observed in CMS4 PDXs (Pearson,  $R = 0.6798$ ,

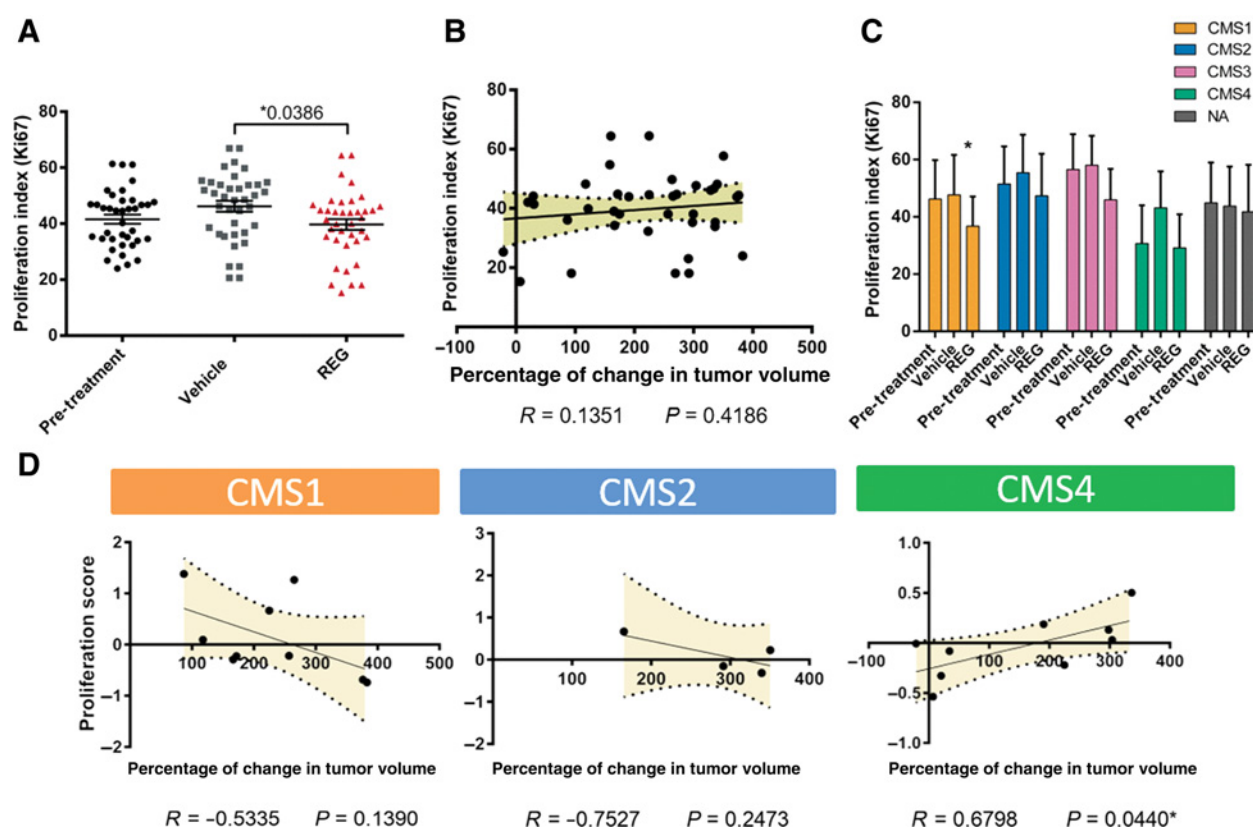


**Figure 2.**

Gene-based proliferation score is a predictor of REG response in CMS4 PDXs. **A**, Ki-67 staining of pre- and post-treatment tumor material reveals that after 4 weeks REG-treated tumors have lower proliferation than the vehicle-treated tumors ( $n = 38$  vehicle,  $n = 38$  REG,  $P = 0.0386$ ). **B**, Post-treatment Ki67 expression does not correlate with changes in PDX tumor volume. **C**, REG effects on tumor cell proliferation determined by Ki-67 staining, analyzed according to CMS subtypes. Mean is presented for each subtype (CMS1  $n = 10$ , CMS2  $n = 3$ , CMS3  $n = 2$ , CMS4  $n = 9$ , N/A  $n = 14$ ). Error bars indicate SEM. **D**, Gene-based proliferation gene score generated from historical PDX gene expression (REG-naïve) data (GSE76402) does not correlate with later therapeutic response in CMS1 ( $n = 9$ ,  $P = 0.1390$ ) or CMS2 ( $n = 4$ ,  $P = 0.2473$ ) PDXs. A significant ( $n = 9$ ,  $R = 0.6798$ ,  $P = 0.0440$ ) linear correlation between gene-based proliferation score percentage of change in tumor volumes indicates that the proliferative score may predict tumor response in the CMS4 subtype.

$P = 0.0440$ ; Fig. 2C), highlighting the potential utility of tumor proliferation capacity score as a predictor of response in CMS4 tumors. No significant correlation was observed between PDX proliferation score and CNA cluster (Supplementary Fig. S2C).

#### DR\_MOMP identifies PDX susceptibility to genotoxic stress and predicts REG response in the CMS4 subtype

REG is known to affect apoptotic pathways through activation of the BH3-only protein PUMA (5). Thus, we next used the systems-based tool, DR\_MOMP, to determine whether the predicted sensitivity of a PDX model to undergo MOMP (and thus, apoptosis) was related to the observed REG response. To generate input data for the DR\_MOMP model, quantitative Western blots were performed using FF REG-naïve tumor material from the  $n = 43$  pre-treatment PDX models. Absolute protein levels of BAK, BAX, BCL-2, BCL-xL, and MCL-1 were determined (Supplementary Figs. S3–S6; Fig. 3A and B). Using these data, DR\_MOMP calculates a numerical value for each PDX model (based on the predicted levels of BH3-only proteins required to induce MOMP), indicating how resistant or sensitive it is to MOMP induction, and therefore to apoptosis (29). The higher the calculated “stress-dose” required to induce MOMP, the more apoptosis resistant the tumor is predicted to be. Although quantified levels of BCL-2 family proteins varied between subtypes, there were no CMS or CNA subtype-specific differences in the stress-dose required to induce MOMP when apoptosis sensitivity was estimated at a systems level ( $P \geq 0.05$  across all groups; Fig. 3C and D). To determine whether the calculated stress-dose required to induce MOMP could be used as a predictive marker of tumor response to REG in specific CMS subtypes, correlation analysis was performed (Fig. 3E). No significant correlation was observed in CMS1 or 2. As noted previously, the ability of DR\_MOMP to predict REG response could not be analyzed in the CMS3 subtype due to a low number of CMS3 PDX models. In CMS4 PDX models, a significant positive correlation between the predicted stress-dose required to induce MOMP and tumor growth was apparent ( $r = 0.7013$ ;  $P = 0.0353$ ). This highlights the potential utility of DR\_MOMP as a predictor of REG response within CMS4. When analyzed in the context of CNA clusters, a significant positive correlation was also seen between the predicted stress-dose required to induce MOMP and PDX tumor volume in CNA high cluster 3 ( $r = 0.6056$ ;  $P = 0.0006$ ; Fig. 3F).

#### RPPA analysis identifies proteomic clusters of distinct activated/deactivated signaling pathways

To provide hints toward novel contexts of vulnerability and future REG combination approaches, we next used an RPPA approach to explore whether REG treatment responses were related to differences in cell signaling pathways before treatment. We generated RPPA data for 72 signaling phospho-proteins from 39 of the 43 FF REG-naïve pretreatment PDX samples (4 samples were removed due to poor quality). The phospho-proteins chosen are involved in several key pathways, including cell proliferation, invasiveness signaling, energetics/hypoxia, and apoptosis/DNA repair/stress signaling. First, we performed unsupervised consensus clustering on the RPPA data, which identified four distinct RPPA clusters, termed C1, C2, C3, and C4, based on the protein profiles. Clusters C1–4 contained 6, 17, 14, and 2 PDX models, respectively (Fig. 4A). We found that samples in RPPA cluster C1 showed significantly higher mean levels of proteins involved in cell proliferation, including phosphorylated MAPK kinase 1/2 (MEK1/20S217), RAC-alpha serine/threonine-protein kinase (AKT), and phosphorylated S6K-alpha-1 (RSK

S380) compared with clusters C2, C3, and C4 (ANOVA and Tukey's *post hoc*,  $P < 0.05$ ). Samples in RPPA cluster C2 showed higher mean levels of pro-apoptotic protein Pro-Caspase-3 compared with clusters C1, C3, and C4 (ANOVA and Tukey *post hoc*,  $P < 0.05$ ). Samples in RPPA cluster C3 were found to have greater mean levels of the pro-apoptotic protein BAX, along with proteins involved in proliferation (MEK-1) and phosphorylated cyclin-dependent kinase inhibitor 1B ([p27]T157) compared with clusters C1, C2, and C4 (ANOVA and Tukey *post hoc*,  $P < 0.05$ ). In contrast, we found significantly lower mean phosphorylated STAT3(Y705) levels in C3 compared with C1, C2, and C4. RPPA cluster C4 was not significantly associated with any proteins due to its low number of samples ( $n = 2$ ).

Next, we investigated whether the RPPA clusters were associated with response to REG. RPPA cluster C2 was found to contain all of the PDX models that displayed stable disease upon REG treatment, that is, non-progressors ( $n = 6$ ), although C2 also contained progressive disease models ( $n = 11$ ). In contrast, C1, C3, and C4 contained only PDX models that progressed under REG treatment ( $n = 22$ ; Fig. 4B i). Examination of the CMS subtypes of models present in RPPA cluster C2 revealed that 4 samples belonged to CMS1 (from a total 8 CMS1 cases), 5 to CMS4 (from a total 9 CMS4 cases), and 8 were unassigned (from a total of 17 CMS-unassigned cases; Fig. 4B ii). Of the 6 C2 non-progressor models, 4 were CMS4, whereas 2 were of unassigned CMS subtype. None of the 4 C2 models that were categorized as CMS1 responded to treatment (Fig. 4B ii). There were 4 CMS4 models present in clusters C3 and C4 that showed no response to REG.

We sought to further characterize the biology underpinning response to REG by analyzing the interaction between CMS subtypes and RPPA clusters in REG-naïve PDX models. To this end, we fitted a classification decision tree to predict response to REG [stabilization (i.e., non-progression) vs. progression] in the available 39 PDX models assigned to both a CMS subtype (CMS1–4 or unassigned) and an RPPA cluster (C1–4). The trained decision tree could discriminate non-progressor REG-treated PDX models (4 out of 6, 67% specificity) from progressor REG-treated PDX models (32 out of 33, 97% sensitivity) with 92% overall accuracy. We observed similar performance (overall accuracy: 90%, specificity: 67%, sensitivity: 94%) when assessing classification metrics from a leave-one-out cross-validation scheme, confirming the robustness of our results. The classification decision tree (Fig. 4C) highlights how PDXs from RPPA clusters C1, C3, and C4 (22 out of 39, 56%) were predicted to progress (0% actual stabilization). Similarly, PDXs from C2 with CMS subtypes CMS1 or unassigned (12 out of 39, 31%) were predicted to progress (2 out of 12, 17% actual stabilization). In contrast, PDXs from C2 with CMS subtypes CMS2–4 (5 out of 39, 13%) were predicted to stabilize (4 out of 5, 80% actual stabilization).

We also analyzed the identified CNA clusters in the context of RPPA clusters. The CNA clusters were equally distributed among RPPA clusters C1–C4 (Fisher test,  $P < 0.62$ ; Fig. 4A). However, 5 of the 6 C2 samples that displayed disease stabilization with REG treatment were in CNA high cluster 3. The remaining PDX models in RPPA C2 were in CNA intermediate cluster 2 (Fisher test,  $P < 0.7$ ; Fig. 4B iii).

Finally, we performed an analysis of individual proteins associated with treatment response to REG, independent of any cluster allocation, using predictive analysis of microarray. We found cleaved Caspase-9, Baculoviral IAP repeat-containing protein 2 (C-IAP1), and BCL-2 (T56) levels to be significantly associated with response to REG

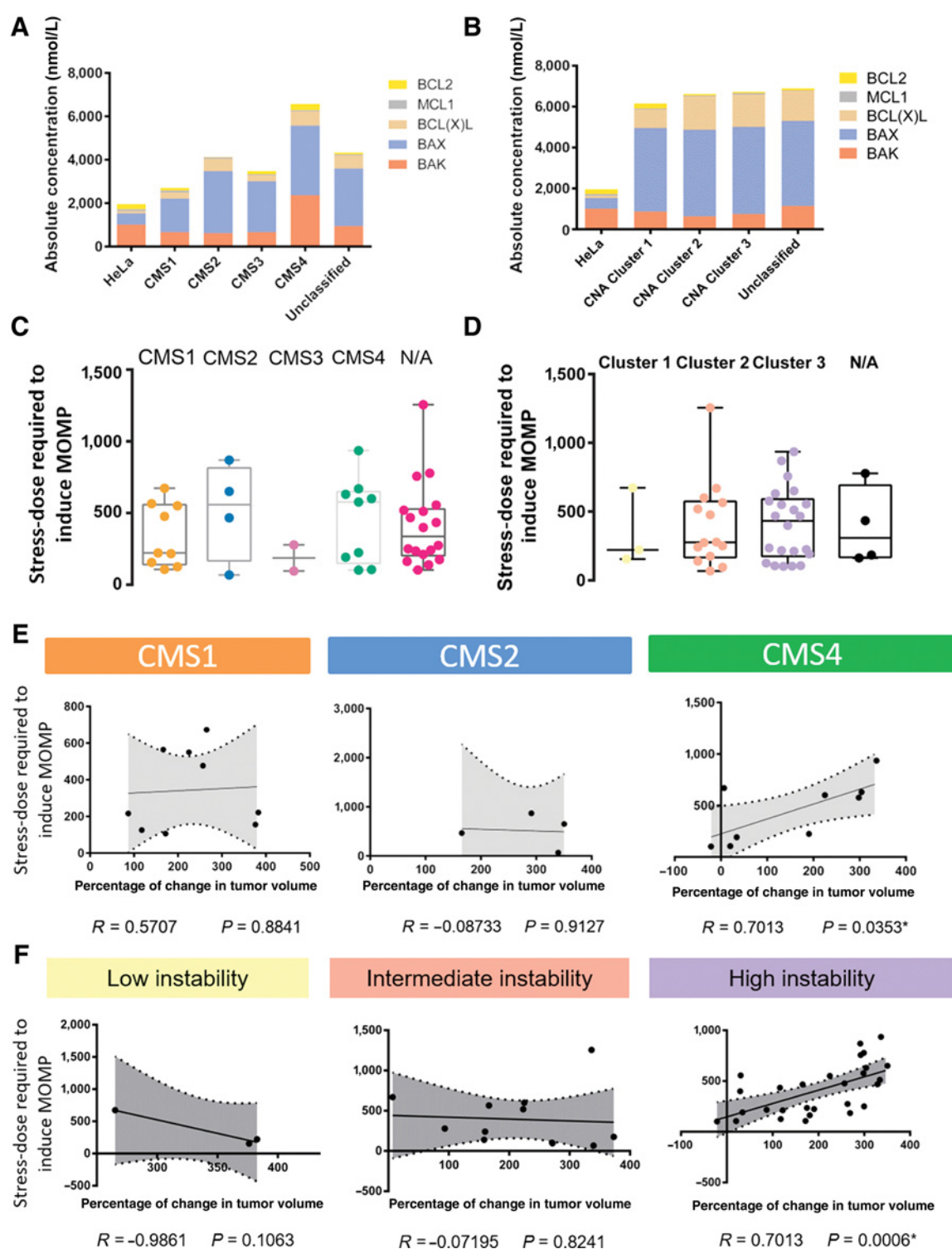
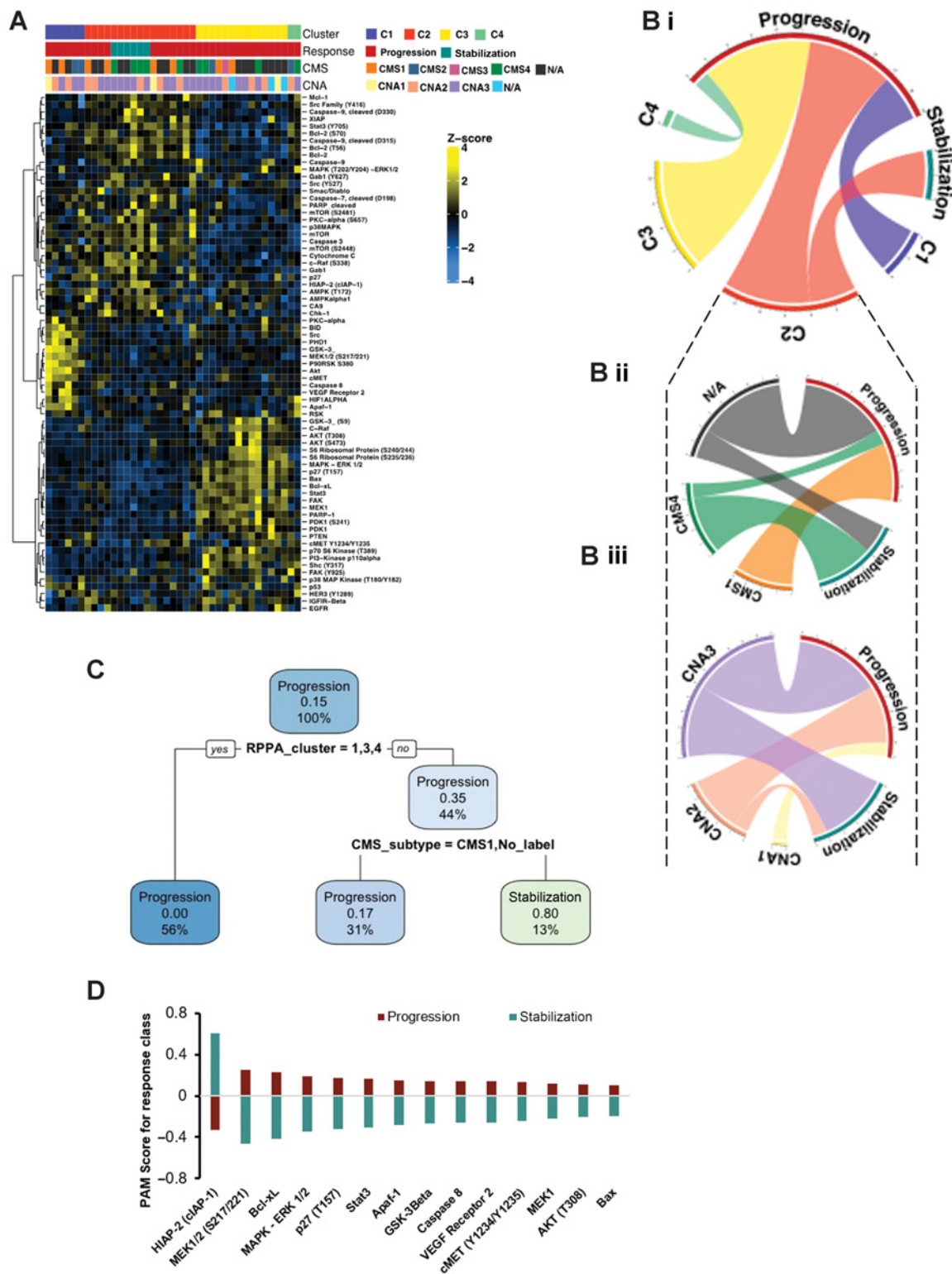


Figure 3.

Apoptosis sensitivity score is a predictor of REG outcome in CMS4 and CNA high subtyped mCRC PDX models. **A** and **B**, Absolute concentrations of BCL2 family proteins were quantified in pre-treatment PDX models ( $n = 43$ ) for each CMS subtype (**A**) and CNA cluster (**B**; displayed as mean expression per group). **C** and **D**, Calculated apoptosis sensitivity scores for each CMS subtype (**C**) and CNA cluster (**D**). **E**, Apoptosis sensitivity score does not correlate with therapeutic outcome in CMS1 ( $n = 9$ ) or CMS2 ( $n = 4$ ) PDXs. A significant  $n = 9$  linear correlation between apoptosis sensitivity score and change in tumor volume indicates that the apoptosis sensitivity score may predict tumor outcome in the CMS4 subtype. **F**, Stress-dose required to induce MOMP does not correlate with therapeutic outcome in CNA low cluster 1 ( $n = 3$ ) or CNA intermediate cluster 2 ( $n = 12$ ) PDXs. A significant ( $n = 27$ ,  $R = 0.7013$ ,  $P = 0.0006^*$ ) linear correlation between the predicted stress-dose required to induce MOMP and change in tumor volume predicts response in CNA high cluster 3 PDXs.



**Figure 4.** RPPA analysis reveals four phospho-protein clusters. **A**, Heatmap showing the level of phospho-proteins as determined by RPPA. PDX models were annotated with cluster number, response to REG, CMS subtype, and CNA cluster information. **B**, Chord diagrams show overlap between RPPA clusters and response to REG. Chord diagrams **B ii** and **iii** shows the CMS subtype (**B ii**) and CNA cluster (**B iii**) information for PDXs grouped into RPPA cluster C2. **C**, Classification decision tree trained on assignments from RPPA clusters and CMS subtyping predicts response to REG treatment. Each node is annotated with the predicted treatment response (stabilization vs. progression), purity (probability of response), and percentage of samples. **D**, Bar plot showing proteins predicting response to treatment in RPPA cluster C2 as determined by PAM.

Downloaded from <http://aacrjournals.org/clinccancerres/article-pdf/27/21/1597/92989536/5979.pdf> by guest on 09 March 2022

(Supplementary Fig. S7). Furthermore, when analysis was limited to the 17 PDX models of RPPA cluster C2, C-IAP1, MEK1/2, and BCL-xL levels were significantly associated with response to treatment (Fig. 4D).

### Supervised transcriptomic analysis identifies genes associated with REG therapeutic response

#### Transcriptomic analysis of post-treatment PDX models

Finally, to interrogate a putative subtype-specific REG mechanism of action, we used kinase outlier analysis (38). Post-treatment tumor material from the previously identified progressor [ $n = 3$  (all CMS1) and non-progressor ( $n = 5$ ;  $n = 3$  CMS4,  $n = 2$  CMS unclassified)] mice were initially used in this analysis. Vehicle control- and REG-treated PDX material was processed for RNA sequencing, which was performed at a depth of 50 million reads. Unsupervised clustering revealed >300 genes that were differentially expressed between non-progressor and progressor PDX models ( $P \leq 0.05$ ;  $-2.0 \geq x \geq +2.0$ ; data not shown). Subsequent supervised clustering, revealed that of known REG targets, *UGT1A1*, *MAPK11*, *EPHA2*, and *CYP2B6* were differentially expressed in non-progressor versus progressor models. *UGT1A1*, *MAPK11*, and *EPHA2* were more highly expressed in the models that progressed whereas *CYP2B6* was expressed more highly in the non-progressor models (Fig. 5A).

#### Supervised analysis of (REG-naïve) PDX expression data

Using supervised outlier analysis of PDX microarray data [previously generated from earlier passages of the same PDX models (i.e., REG naïve); transcriptomic data available at GSE76402], we next sought to investigate whether basal expression of the REG targets identified in the supervised analysis could predict later outcome to REG therapy. We found that only *EPHA2* was differentially expressed at a basal level in REG-naïve PDXs. Further analysis revealed a significant positive linear correlation between basal *EPHA2* expression values and later treatment outcome within the entire PDX cohort [Fig. 5B;  $R = 0.3116$ ; 95% CI, 0.008425–0.5624;  $P = 0.0445$ ].

To determine whether differential transcriptomic changes were also evident at the protein level, and to further validate these findings, we performed Western blot analysis using available PDX tissue taken pre- and post-REG treatment. WB analysis confirmed that pre- and post-treatment *EPHA2* protein expression is higher in PDX models that progressed following REG treatment compared with non-progressor models (Supplementary Fig. S8).

## Discussion

To our knowledge, this is the first multilayered preclinical biomarker study to adopt functional, pathway-, and systems-based multi-omic analyses to simultaneously interrogate the putative role of novel colorectal cancer subtypes as biomarkers for REG. Here, we have shown that PDX models replicate a subtype-specific drug response observed in the hypothesis-generating retrospective analysis of CORRECT trial data, where CMS4 patients show best response to REG treatment (19, 20). Moreover, data from PDXs with intermediate/high CNA profiles suggest a favorable response to REG. We observed that tumor proliferation capacity score (using a pre-established 11-gene “proliferation signature”) as well as apoptosis sensitivity were predictive of overall tumor response to REG in CMS4 PDXs ( $P = 0.044$  and  $P = 0.035$ , respectively). RPPA analysis revealed four phospho-protein-based clusters. Only cluster

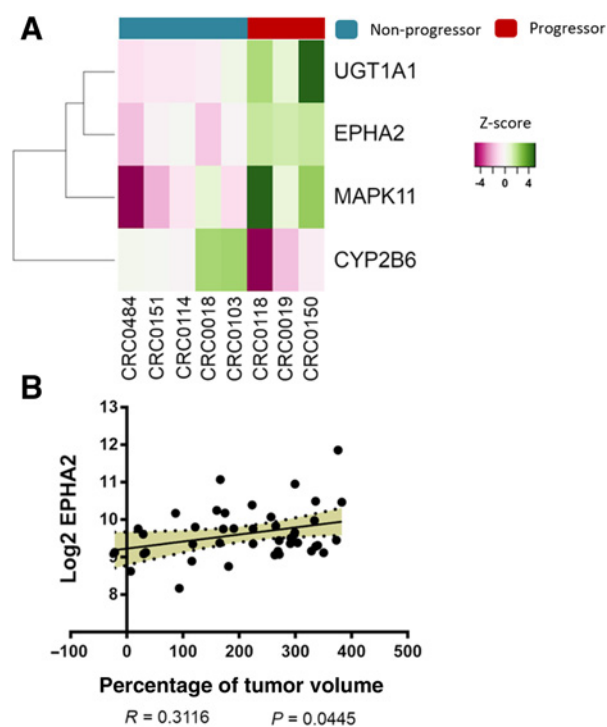


**Figure 5.**

Expression outlier analysis reveals differential profiles of key REG target genes in CMS4/NA (REG non-progressor) versus CMS1 (REG progressor) PDX models. **A**, Supervised hierarchical clustering identifies differential expression of key REG targets in post-treatment CMS4/unassigned REG non-progressor models ( $n = 5$ ) versus CMS1 ( $n = 3$ ) REG progressor PDX models. **B**, A significant ( $n = 41$   $R = 0.3116$ ,  $P = 0.0445$ ) linear correlation between basal *EPHA2* expression [identified from mining of historical (REG-naïve) PDX gene expression data (GSE76402)] and the effect of REG on tumor volume indicates that *EPHA2* expression may predict tumor response to REG irrelevant of the CMS subtype.

C2 contained REG-responsive models, which were also characterized by a significantly higher level of Pro-Caspase-3. A classification decision tree identified a sub-population of PDXs composed of cluster C2 and subtypes CMS2–4 enriched for REG non-progressors. Finally, differential gene expression analysis of post-treatment tumors (best and worst responders) revealed a potential role for *EPHA2* in mediating resistance to REG. Its potential utility as a predictive biomarker of REG response was revealed through analysis of basal gene expression levels.

A PDX population study was implemented, with models selected to reflect both the incidence of mutations in the global human colorectal cancer population while also considering CMS. The  $1 \times 1$  experimental approach using mRECIST criteria has previously been shown to effectively facilitate the assessment of drug response across a large number of models to determine population-based response rates (36). REG response was not related to the mutation status of PDXs. Analysis by CMS subtype revealed that REG effects on tumor growth delay recapitulated the hypothesis-generating results observed by Teufel and colleagues (19) in the clinical setting. However, we note that modest disease control was the best observed response in the PDX trial and that REG treatment caused disease stabilization/progression in the PDX cohort at a similar frequency to that reported in a retrospective study of REG-treated patients with mCRC (39).

Previously, we identified three distinct patient subgroups based on CNA profiles that were able to predict outcome to bevacizumab combination treatment (14). This work further suggested an overlap between CMS subtypes and CNA clusters, with enrichment of CMS1/3 in CNA low cluster 1 and enrichment of CMS2/4 in CNA intermediate cluster 2 and CNA high cluster 3 (14). The overlap between CNA clusters and CMS subtypes provides an insight into the biological characteristics that may underpin this response. CMS2 tumors have been found to have more frequent copy-number gains in oncogenes and copy-number losses in tumor-suppressor genes (40). Evidence suggests a link between chromosomal instability and a chronically inflamed tumor microenvironment (41, 42). Indeed, the mesenchymal CMS4 subtype is characterized by tumors with a high CNA load and a pro-angiogenic, inflammatory immunosuppressed environment (16, 43). Therefore, it is possible that tumors characterized by high chromosomal instability (i.e., CNA cluster 2 and 3) and an inflamed microenvironment, may benefit from treatment with REG. Supporting this hypothesis, all PDXs ( $n = 3$ ) assigned to CNA low cluster 1 progressed under REG treatment. However, the low sample numbers in cluster 1 are acknowledged and further studies are required to confirm this effect.

We next sought to determine whether the positive effect of REG observed in CMS4-subtyped PDXs was mediated through an anti-angiogenic effect. Following 28 days of treatment, CD31 expression across the entire PDX cohort was lower in REG-treated compared with vehicle-treated PDX tumors (Fig. 1C and D). Although there was a significant decrease in CD31 expression in CNA low cluster 1 tumors (Supplementary Fig. S2A), limited conclusions can be drawn due to the small sample size in this cluster. Moreover, as these tumors are largely resistant to treatment this effect is unlikely to be of significant mechanistic relevance. Our data suggest that the observed putative REG subtype-specific activity is unlikely to be mediated by a differential anti-angiogenic response.

It has been well documented that REG inhibits proliferation in tumor cells through inhibition of MAPK and ERK signaling (44, 45). Here, this effect is also observed across our PDX cohort (Fig. 2A;  $P = 0.0386$ ). Subtype-dependent analysis revealed that Ki-67 expression post-treatment was significantly lower in REG-treated CMS1 tumors compared with CMS1 vehicle controls, yet average responses were numerically similar across all CMS subtypes. To investigate whether antiproliferative activity was predictive of REG responses overall and between subtypes, we analyzed an 11-gene proliferation signature using REG-naïve PDX gene expression data (28). Our analysis revealed a significant ( $P = 0.044$ ) correlation between change in tumor volume and proliferation capacity score within the CMS4 subtype. CMS4 tumors with a low proliferation capacity score displayed disease stabilization whereas CMS4 tumors with a high proliferation capacity score displayed disease progression. Conversely, no significant correlations were observed between change in tumor volume and proliferation capacity score in CMS1. As observed in previous clinical studies (19, 20), tumors assigned to CMS1 received no benefit from REG therapy. Despite enrichment of BRAF mutations [Fig. 3D; in Guinney and colleagues (16)], there is heterogeneity in oncogenic/cell proliferation pathways in the CMS1 subtype. Such heterogeneity was similarly observed in the current study. The low number of CMS3 PDXs precluded meaningful assessment of the predictive capability of the gene-based proliferation signature in this subtype. We note that the accuracy of CMS3 classification is generally low, highlighting inherent difficulties with correlative analyses in this subtype (21).

As REG is also known to affect apoptotic pathways (5), we next sought to investigate whether this cancer hallmark effect was related to tumor subtype. We used a validated systems biology model of apoptosis (DR\_MOMP; refs. 29, 46, 47) to predict tumor sensitivity to undergo apoptosis following treatment. A significant positive correlation between the predicted stress-dose required to induce MOMP and PDX treatment response was seen in CMS4 tumors, and in tumors assigned to CNA high cluster 3. Specifically, CMS4 tumors predicted to be apoptosis resistant (and to require a higher stress-dose to induce MOMP) were less vulnerable to REG treatment, compared with those predicted to be apoptosis sensitive (and to require a lower stress-dose to induce MOMP). This correlation was not evident in CMS1 or CMS2 tumors. Moreover, given the previously identified overlap of the CMS4 subtype with CNA high cluster 3 (14), DR\_MOMP was also predictive in this CNA cluster. Previous studies have shown that REG-induced upregulation of the BH3-only protein PUMA promotes chemosensitization and apoptosis in colorectal cancer cell lines (5). Although our results highlight the potential utility of DR\_MOMP as a predictor of response to REG within the CMS4 subtype, our data also suggest that apoptosis could be a key targetable pathway in CMS4 tumors. For example, CMS4 tumors with a high DR\_MOMP score could benefit from a REG combination with a BCL2 antagonist. The proliferation and apoptosis signatures presented, which identifies REG non-progressors within the CMS4 subtype, are amenable to the molecular pathology setting, and could serve as stratification tools for REG in the clinic.

Signaling pathway status in PDX models was studied by RPPA, a sensitive method that can detect levels of phospho-proteins (48). Among the identified RPPA clusters, we observed that non-progressor PDX models were only evident in cluster C2. The PDX models in RPPA cluster C2 were hallmarked by a significantly higher level of Pro-Caspase-3. Although we did not have the CMS status for 8 of the 17 PDX models of C2, 44% of the defined models were CMS1 and 56% CMS4. Interestingly, 4 of the 5 CMS4 tumors in RPPA cluster C2 responded to REG. In contrast, the remaining 4 CMS4 models (found in the RPPA cluster C3 and C4) showed no response to REG, suggesting that almost exclusively, CMS4 tumors of the RPPA C2 subtype are responsive to REG. The CMS4 subtype is characterized by higher level of TGF- $\beta$  signaling, angiogenesis, complement activation as well as stromal infiltration and immune upregulation (16). We also observed that the CMS4 subtype within RPPA cluster C2 compared with CMS4 in other clusters have differences in protein level of PCNA-interacting partner (PARI; PARP-1), Caspase-3, and serine/threonine-protein kinase mTOR, suggesting that further studies based on these individual proteins might be useful to model the REG response. Moreover, RPPA cluster C2 also contained a higher proportion of CNA intermediate cluster 2 and CNA high cluster 3 tumors (94% in C2 compared with 84% overall). These observations suggest that together, CMS4 subtype, a high CNA burden, and a low predicted stress-dose required to induce MOMP could be predictive for response to REG. These data require further validation in a larger cohort due to the low sample size in CNA low cluster 1 ( $n = 3$ ).

To interrogate subtype-specific REG mechanism of action, post-treatment PDX tumors (from both REG- and vehicle-treated best and worst responders) from the 5 models identified as non-progressors ( $n = 3$  CMS4 and  $n = 2$  CMS unassigned) and 3 models identified as progressors (CMS1) were subjected to gene expression analysis. Supervised clustering revealed that known REG targets *UGT1A1*, *MAPK11*, and *EPHA2* were more highly expressed in the models that progressed whereas *CYP2B6* was expressed more highly in models that did not progress following treatment. Next, gene expression analysis

of the identified targets (*UGT1A1*, *MAPK11*, *EPHA2*, and *CYP2B6*) was performed using available microarray data (GSE76402, open access) from the same cohort of PDX tumors (i.e., to investigate basal levels of gene expression in REG-naïve tumor material). *EPHA2* was found to be differentially expressed across the PDXs at a basal level. Subsequent correlation analysis revealed that *EPHA2* expression values were positively correlated with models that were resistant to REG (Fig. 5). These findings were validated by Western blot analysis of *EPHA2* protein in the same PDX models. *EPHA2* is a known target of REG (4) and has been shown to modulate angiogenesis and metastasis in several cancers (49–51). Moreover, it has been associated with poor outcome and has been implicated in resistance to FOLFIRI + cetuximab combination therapy in colorectal cancer (52). The *EPHA2* tyrosine kinase receptor has been implicated in tumor progression, stemness, and resistance to treatment in a number of cancers (53). Moreover, disruption of *EPHA2* signaling in preclinical models of non-small cell lung cancer and mCRC has been shown to impair tumor cell proliferation, and viability while inducing apoptosis (54, 55). It is possible that REG may convey a therapeutic benefit in CMS4 through such mechanisms, and that increased expression of *EPHA2* could be a potential resistance mechanism in patients that progress following REG treatment. Although expression levels of *EPHA2* may predict REG outcome in CMS4 tumors, these data also suggest that REG delivered in combination with a novel *EPHA2* inhibitor (e.g., GLPG1790; ref. 53) or of an *EPHA2*-targeted nanotherapeutic (56) could improve response. REG has previously been shown to inhibit *EPHA2* in the *in vitro* setting (110–240 nmol/L; ref. 4). Further studies are now mandated to establish the role of *EphA2* kinase domain mutations in mediating REG-induced *EPHA2* inhibition. Clinical validation of *EPHA2* as a predictive biomarker and/or therapeutic target is also warranted.

Overall, functional and multi-omic analyses suggest that CMS4 and CNA high tumors may respond best to REG. Within the context of CMS4, we have presented data that support further development of an apoptotic/proliferation signature to predict REG response. We have also shown that tumors classified into CMS4 and RPPA subtype C2 are almost exclusively non-progressors when treated with REG. In addition, we have presented a classification decision tree that predicts response to REG with higher accuracy by integrating the signaling pathways cross-talk recapitulated by the RPPA clusters and the CMS subtyping. Collectively, our data suggest that a combination of protein and gene expression subtyping identifies the vast majority of non-progressors. Finally, we have shown that *EPHA2* may be involved in a mechanism of resistance to REG. We acknowledge that use of PDX models (established in immunocompromised mice) precludes assessment of the immunomodulatory effects of REG (8). Additional studies are required to unravel these mechanisms. Overall (and as discussed elsewhere; ref. 21), our data provide evidence that CMS and other subtype classification systems should not be used as a “one fits all tool,” but should rather represent canonical “*termini a quo*” to (i) deepen knowledge of colorectal cancer biology, (ii) support biomarker identification, and (iii) provide a platform to identify novel contexts of vulnerability. Including functional characterization of biological systems may also optimize the biomarker identification process, especially for multi-targeted MKIs where one single biomarker entity is unlikely to exist.

### Authors' Disclosures

A. Lafferty reports grants from Science Foundation Ireland during the conduct of the study. A.C. O'Farrell reports grants from Science Foundation Ireland and European Union's Horizon 2020 during the conduct of the study. G. Argilés reports

personal fees from Bayer, Servier, and Roche; grants and personal fees from Amgen; grants from Merck Serono; and personal fees from Sanofi outside the submitted work. J. Tabernero reports personal fees from Array Biopharma, AstraZeneca, Avvinity, Bayer, Boehringer Ingelheim, Chugai, Daiichi Sankyo, F. Hoffmann-La Roche Ltd., Genentech Inc, HaliDX SAS, Hutchison MediPharma International, Ikena Oncology, IQVIA, Lilly, Menarini, Merck Serono, Merus, MSD, Mirati, Neophore, Novartis, Orion Biotechnology, Peptomyc, Pfizer, Pierre Fabre, Samsung Bioepis, Sanofi, Seattle Genetics, Servier, Taiho, Tessa Therapeutics, TheraMyc, Imedex, Medscape Education, MJH Life Sciences, PeerView Institute for Medical Education, and Physicians Education Resource (PER) outside the submitted work. R. Dienstmann reports personal fees from Roche, Boehringer Ingelheim, Merck Sharp & Dohme, Amgen, Ipsen, Sanofi, Servier, and Libbs, as well as grants from Merck and Pierre Fabre outside the submitted work. L. Trusolino reports grants from Symphogen, Servier, Pfizer, Menarini, Merus, and Merck KGaA, as well as personal fees from AstraZeneca, Merck KGaA, and Eli Lilly outside the submitted work. A.T. Byrne reports grants from Science Foundation Ireland and European Union's Horizon 2020 research and innovation programme during the conduct of the study. No disclosures were reported by the other authors.

### Authors' Contributions

**A. Lafferty:** Data curation, formal analysis, investigation, visualization, methodology, writing—original draft, writing—review and editing. **A.C. O'Farrell:** Supervision, investigation, visualization, writing—original draft, project administration, writing—review and editing. **G. Migliardi:** Formal analysis, supervision, investigation, writing—review and editing. **N. Khemka:** Data curation, formal analysis, investigation, visualization, writing—original draft, writing—review and editing. **A.U. Lindner:** Data curation, formal analysis, investigation, writing—review and editing. **F. Sassi:** Resources, investigation, methodology, writing—review and editing. **E.R. Zanella:** Resources, supervision, writing—review and editing. **M. Salvucci:** Data curation, formal analysis, investigation, writing—original draft, writing—review and editing. **E. Vanderheyden:** Investigation, methodology, writing—review and editing. **E. Modave:** Data curation, formal analysis, investigation, writing—review and editing. **B. Boeckx:** Data curation, formal analysis, investigation, writing—review and editing. **L. Halang:** Investigation, writing—review and editing. **J. Betge:** Resources, data curation, writing—review and editing. **M.P.A. Ebert:** Resources, data curation, writing—review and editing. **P. Dicker:** Data curation, formal analysis, writing—review and editing. **G. Argilés:** Resources, writing—review and editing. **J. Tabernero:** Resources, writing—review and editing. **R. Dienstmann:** Resources, funding acquisition, writing—review and editing. **E. Medico:** Resources, supervision, funding acquisition, writing—review and editing. **D. Lambrechts:** Resources, formal analysis, supervision, investigation, writing—review and editing. **A. Bertotti:** Resources, data curation, formal analysis, supervision, funding acquisition, methodology, writing—review and editing. **C. Isella:** Resources, data curation, supervision, writing—review and editing. **L. Trusolino:** Conceptualization, resources, data curation, supervision, funding acquisition, methodology, writing—review and editing. **J.H.M. Prehn:** Conceptualization, resources, supervision, funding acquisition, visualization, methodology, writing—original draft, writing—review and editing. **A.T. Byrne:** Conceptualization, resources, supervision, funding acquisition, visualization, methodology, writing—original draft, project administration, writing—review and editing.

### Acknowledgments

This research was supported by a Science Foundation Ireland (SFI) Career Development Award “Coloforetell” (grant agreement number: 13/CDA/2183; to A.T. Byrne). Additional funding was from AIRC. Associazione Italiana per la Ricerca sul Cancro, Investigator Grants 20697 (to A. Bertotti), 12944 (to E. Medico), and 22802 (to L. Trusolino); AIRC 5 × 1,000 grant 21091 (to A. Bertotti, E. Medico, and L. Trusolino); AIRC/CRUK/FC AECC Accelerator Award 22795 (to L. Trusolino); My First AIRC grant 19047 (to C. Isella); European Research Council Consolidator Grant 724748—BEAT (to A. Bertotti); and Fondazione Piemontese per la Ricerca sul Cancro-ONLUS, 5 × 1,000 Ministero della Salute 2015 (to E. Medico and L. Trusolino), 2014 and 2016 (to L. Trusolino). J.H.M. Prehn received funding from Science Foundation Ireland and the Health Research Board (14/IA/2582, 16/US/3301). A.T. Byrne, J.H.M. Prehn, L. Trusolino, D. Lambrechts, M.P.A. Ebert, J. Tabernero and R. Dienstmann are further supported by the European Union's Horizon 2020 Health Research and Innovation award “COLOSSUS” (grant agreement number: 754923). A.T. Byrne, L. Trusolino, E. Medico and A. Bertotti are members of the EurOPDX Consortium, and receive funding from the European Union's Horizon 2020 research and innovation program, grant agreement no. #731105 (EurOPDX Research Infrastructure, www.europdx.eu). We are grateful

to Bayer Healthcare for providing REG. We thank Dr. Sandra Van Schaebroeck for advice regarding EPHA2 Western blot antibody.

The costs of publication of this article were defrayed in part by the payment of page charges. This article must therefore be hereby marked

*advertisement* in accordance with 18 U.S.C. Section 1734 solely to indicate this fact.

Received March 12, 2021; revised July 5, 2021; accepted August 18, 2021; published first August 23, 2021.

## References

- Fondevila F, Méndez-Blanco C, Fernández-Palanca P, González-Gallego J, Mauriz JL. Anti-tumoral activity of single and combined regorafenib treatments in preclinical models of liver and gastrointestinal cancers. *Exp Mol Med* 2019;51:109.
- Grothey A, Van Cutsem E, Sobrero A, Siena S, Falcone A, Ychou M, et al. Regorafenib monotherapy for previously treated metastatic colorectal cancer (CORRECT): an international, multicentre, randomised, placebo-controlled, phase 3 trial. *Lancet* 2013;381:303–12.
- Li J, Qin S, Xu R, Yau TC, Ma B, Pan H, et al. Regorafenib plus best supportive care versus placebo plus best supportive care in Asian patients with previously treated metastatic colorectal cancer (CONCUR): a randomised, double-blind, placebo-controlled, phase 3 trial. *Lancet Oncol* 2015;16:619–29.
- Wilhelm SM, Dumas J, Adnane L, Lynch M, Carter CA, Schutz G, et al. Regorafenib (BAY 73–4506): a new oral multikinase inhibitor of angiogenic, stromal and oncogenic receptor tyrosine kinases with potent preclinical anti-tumor activity. *Int J Cancer* 2011;129:245–55.
- Chen D, Wei L, Yu J, Zhang L. Regorafenib inhibits colorectal tumor growth through PUMA-mediated apoptosis. *Clin Cancer Res* 2014;20:3472–84.
- Arai H, Battaglin F, Wang J, Lo JH, Soni S, Zhang W, et al. Molecular insight of regorafenib treatment for colorectal cancer. *Cancer Treat Rev* 2019;81:101912.
- Abou-Elkacem L, Arns S, Brix G, Gremse F, Zopf D, Kiessling F, et al. Regorafenib inhibits growth, angiogenesis, and metastasis in a highly aggressive, orthotopic colon cancer model. *Mol Cancer Ther* 2013;12:1322–31.
- Hoff S, Grünewald S, Röse L, Zopf D. Immunomodulation by regorafenib alone and in combination with anti-PD1 antibody on murine models of colorectal cancer. *Ann Oncol* 2017;28:v423.
- Tabernero J, Lenz HJ, Siena S, Sobrero A, Falcone A, Ychou M, et al. Analysis of circulating DNA and protein biomarkers to predict the clinical activity of regorafenib and assess prognosis in patients with metastatic colorectal cancer: a retrospective, exploratory analysis of the CORRECT trial. *Lancet Oncol* 2015;16:937–48.
- Lambrechts D, Köchert K, Schulz A, Vonk R, Rutstein M, Kobina S, et al. PD-003 analysis of single-nucleotide polymorphisms (SNPs) in the phase 3 CORRECT trial of regorafenib vs placebo in patients with metastatic colorectal cancer (mCRC). *Ann Oncol* 2016;27:ii102.
- Köchert K, Beckmann G, Teufel M. Exploratory analysis of baseline microsatellite instability (MSI) status in patients with metastatic colorectal cancer (mCRC) treated with regorafenib (REG) or placebo in the phase 3 CORRECT trial. *Ann Oncol* 2017;28:mdx393.060.
- Ducieux M, Petersen LN, Öhler L, Bergamo F, Metges J-P, Groot JW, et al. Outcomes by tumor location in patients with metastatic colorectal cancer (mCRC) treated with regorafenib (REG): final analysis from the prospective, observational CORRELATE study. *J Clin Oncol* 2019;37:539.
- Suenaga M, Mashima T, Kawata N, Wakatsuki T, Horiike Y, Matsusaka S, et al. Serum VEGF-A and CCL5 levels as candidate biomarkers for efficacy and toxicity of regorafenib in patients with metastatic colorectal cancer. *Oncotarget* 2016;7:34811–23.
- Smeets D, Miller IS, O'Connor DP, Das S, Moran B, Boeckx B, et al. Copy number load predicts outcome of metastatic colorectal cancer patients receiving bevacizumab combination therapy. *Nat Commun* 2018;9:4112.
- Singh MP, Rai S, Pandey A, Singh NK, Srivastava S. Molecular subtypes of colorectal cancer: an emerging therapeutic opportunity for personalized medicine. *Genes Dis* 2019;8:133–45.
- Guinney J, Dienstmann R, Wang X, de Reynies A, Schlicker A, Soneson C, et al. The consensus molecular subtypes of colorectal cancer. *Nat Med* 2015;21:1350–6.
- Fridman WH, Miller I, Sautès-Fridman C, Byrne AT. Therapeutic targeting of the colorectal tumor stroma. *Gastroenterology* 2020;158:303–21.
- Martini G, Dienstmann R, Ros J, Baraibar I, Cuadra-Urteaga JL, Salva F, et al. Molecular subtypes and the evolution of treatment management in metastatic colorectal cancer. *Ther Adv Med Oncol* 2020;12:1758835920936089.
- Teufel M, Schwenke S, Seidel H, Beckmann G, Reischl J, Vonk R, et al. Molecular subtypes and outcomes in regorafenib-treated patients with metastatic colorectal cancer (mCRC) enrolled in the CORRECT trial. *J Clin Oncol* 2015;33:3558.
- Vogel A, Hofheinz RD, Kubicka S, Arnold D. Treatment decisions in metastatic colorectal cancer—beyond first and second line combination therapies. *Cancer Treat Rev* 2017;59:54–60.
- Sveen A, Cremolini C, Dienstmann R. Predictive modeling in colorectal cancer: time to move beyond consensus molecular subtypes. *Ann Oncol* 2019;30:1682–5.
- Isella C, Brundu F, Bellomo SE, Galimi F, Zanella E, Porporato R, et al. Selective analysis of cancer-cell intrinsic transcriptional traits defines novel clinically relevant subtypes of colorectal cancer. *Nat Commun* 2017;8:15107.
- Medico E, Bertotti A, Isella C, Bellomo SE, Brundu F, CRIS, a superior predictive and prognostic classification system of colorectal cancer based on high-resolution analysis of cancer cell-autonomous traits II. *Gene Expression Omnibus (GEO): NCBI*; 2015.
- Eide PW, Bruun J, Lothe RA, Sveen A. CMScluster: an R package for consensus molecular subtyping of colorectal cancer preclinical models. *Sci Rep* 2017;7:16618.
- Bertotti A, Migliardi G, Galimi F, Sassi F, Torti D, Isella C, et al. A molecularly annotated platform of patient-derived xenografts (“xenopatients”) identifies HER2 as an effective therapeutic target in cetuximab-resistant colorectal cancer. *Cancer Discov* 2011;1:508–23.
- Beroukhim R, Getz G, Nghiemphu L, Barretina J, Hsueh T, Linhart D, et al. Assessing the significance of chromosomal aberrations in cancer: methodology and application to glioma. *Proc Natl Acad Sci U S A* 2007;104:20007–12.
- Schneider CA, Rasband WS, Eliceiri KW. NIH image to ImageJ: 25 years of image analysis. *Nat Methods* 2012;9:671–5.
- Nielsen TO, Parker JS, Leung S, Voduc D, Ebbert M, Vickery T, et al. A comparison of PAM50 intrinsic subtyping with immunohistochemistry and clinical prognostic factors in tamoxifen-treated estrogen receptor-positive breast cancer. *Clin Cancer Res* 2010;16:5222–32.
- Lindner AU, Concannon CG, Boukes GJ, Cannon MD, Llambi F, Ryan D, et al. Systems analysis of BCL2 protein family interactions establishes a model to predict responses to chemotherapy. *Cancer Res* 2013;73:519–28.
- Xu T, Le TD, Liu L, Su N, Wang R, Sun B, et al. CancerSubtypes: an R/Bioconductor package for molecular cancer subtype identification, validation, and visualization. *Bioinformatics* 2017;33:3131–3.
- Hastie T, Tibshirani R, Nrasimhan B, Chu G. pamr: Pam: Prediction Analysis for Microarrays. R package version 1.56.1. [cited 2020 Oct 21]. Available from: <https://cran.r-project.org/web/packages/pamr/index.html>.
- Tibshirani R, Seo M, Chu G, Narasimhan B, Li J. samr: SAM: significance analysis of microarrays. R package version 3.0. [cited 2020 Oct 21]. Available from: <https://cran.r-project.org/web/packages/samr/index.html>.
- Cuppens T, Moisse M, Depreeuw J, Annibaldi D, Colas E, Gil-Moreno A, et al. Integrated genome analysis of uterine leiomyosarcoma to identify novel driver genes and targetable pathways. *Int J Cancer* 2018;142:1230–43.
- Love MI, Huber W, Anders S. Moderated estimation of fold change and dispersion for RNA-seq data with DESeq2. *Genome Biol* 2014;15:550.
- RCoreTeam. R: a Language and Environment for Statistical Computing 2012. Available from: <https://www.R-project.org>.
- Gao H, Korn JM, Ferretti S, Monahan JE, Wang Y, Singh M, et al. High-throughput screening using patient-derived tumor xenografts to predict clinical trial drug response. *Nat Med* 2015;21:1318–25.
- Motulsky HJ. Prism 4 Statistics Guide - Statistical analyses for laboratory and clinical researchers. GraphPad Software Inc., San Diego CA, 2003. Available from: [www.graphpad.com](http://www.graphpad.com).

38. Medico E, Russo M, Picco G, Cancelliere C, Valtorta E, Corti G, et al. The molecular landscape of colorectal cancer cell lines unveils clinically actionable kinase targets. *Nat Commun* 2015;6:7002.
39. Aljubran A, Elshenawy MA, Kandil M, Zahir MN, Shaheen A, Gad A, et al. Efficacy of regorafenib in metastatic colorectal cancer: a multi-institutional retrospective study. *Clin Med Insights Oncol* 2019;13:1179554918825447.
40. Thanki K, Nicholls ME, Gajjar A, Senagore AJ, Qiu S, Szabo C, et al. Consensus molecular subtypes of colorectal cancer and their clinical implications. *Int Biol Biomed J* 2017;3:105–11.
41. Shivakumar BM, Rotti H, Vasudevan TG, Balakrishnan A, Chakrabarty S, Bhat G, et al. Copy number variations are progressively associated with the pathogenesis of colorectal cancer in ulcerative colitis. *World J Gastroenterol* 2015;21:616–22.
42. Paulson TG, Maley CC, Li X, Li H, Sanchez CA, Chao DL, et al. Chromosomal instability and copy number alterations in Barrett's esophagus and esophageal adenocarcinoma. *Clin Cancer Res* 2009;15:3305–14.
43. Becht E, de Reynies A, Giraldo NA, Pilati C, Buttard B, Lacroix L, et al. Immune and stromal classification of colorectal cancer is associated with molecular subtypes and relevant for precision immunotherapy. *Clin Cancer Res* 2016;22:4057–66.
44. Eschbach RS, Clevert DA, Hirner-Eppeneder H, Ingrisich M, Moser M, Schuster J, et al. Contrast-enhanced ultrasound with VEGFR2-targeted microbubbles for monitoring regorafenib therapy effects in experimental colorectal adenocarcinomas in rats with DCE-MRI and immunohistochemical validation. *PLoS ONE* 2017;12:e0169323.
45. Cyran CC, Kazmierczak PM, Hirner H, Moser M, Ingrisich M, Havla L, et al. Regorafenib effects on human colon carcinoma xenografts monitored by dynamic contrast-enhanced computed tomography with immunohistochemical validation. *PLoS One* 2013;8:e76009.
46. Lindner AU, Salvucci M, Morgan C, Monsefi N, Resler AJ, Cremona M, et al. BCL-2 system analysis identifies high-risk colorectal cancer patients. *Gut* 2017;66:2141–8.
47. Flanagan L, Lindner AU, de Chaumont C, Kehoe J, Fay J, Bacon O, et al. BCL2 protein signalling determines acute responses to neoadjuvant chemoradiotherapy in rectal cancer. *J Mol Med* 2015;93:315–26.
48. Boellner S, Becker K-F. Reverse phase protein arrays-quantitative assessment of multiple biomarkers in biopsies for clinical use. *Microarrays* 2015;4:98–114.
49. Udayakumar D, Zhang G, Ji Z, Njauw CN, Mroz P, Tsao H. EphA2 is a critical oncogene in melanoma. *Oncogene* 2011;30:4921–9.
50. Brantley-Sieders DM, Zhuang G, Hicks D, Fang WB, Hwang Y, Cates JM, et al. The receptor tyrosine kinase EphA2 promotes mammary adenocarcinoma tumorigenesis and metastatic progression in mice by amplifying ErbB2 signaling. *J Clin Invest* 2008;118:64–78.
51. Binda E, Visioli A, Giani F, Lamorte G, Copetti M, Pitter KL, et al. The EphA2 receptor drives self-renewal and tumorigenicity in stem-like tumor-propagating cells from human glioblastomas. *Cancer Cell* 2012;22:765–80.
52. Rey JB, Launay-Vacher V, Tournigand C. Regorafenib as a single-agent in the treatment of patients with gastrointestinal tumors: an overview for pharmacists. *Target Oncol* 2015;10:199–213.
53. Vitiello PP, Mele L, Prisco C, Cardone C, Cardillo D, Poliero L, et al. 28P - GLPG 1790, a new selective EPHA2 inhibitor, is active in colorectal cancer cell lines belonging to the CMS4/mesenchymal-like subtype. *Ann Oncol* 2019;30:v8–v9.
54. Amato KR, Wang S, Hastings AK, Youngblood VM, Santapuram PR, Chen H, et al. Genetic and pharmacologic inhibition of EPHA2 promotes apoptosis in NSCLC. *J Clin Invest* 2014;124:2037–49.
55. Martini G, Cardone C, Vitiello PP, Belli V, Napolitano S, Troiani T, et al. EPHA2 is a predictive biomarker of resistance and a potential therapeutic target for improving antiepidermal growth factor receptor therapy in colorectal cancer. *Mol Cancer Ther* 2019;18:845–55.
56. Kamoun WS, Kirpotin DB, Huang ZR, Tipparaju SK, Noble CO, Hayes ME, et al. Antitumour activity and tolerability of an EphA2-targeted nanotherapeutic in multiple mouse models. *Nat Biomed Eng* 2019;3:264–80.